Supplementary Materials

Enzymes degrading fungal cell-wall components vs those exhibiting lactonase activity as participants of antifungals

Maksim Domnin [1], Aysel Aslanli [1], Olga Senko [1], Nikolay Stepanov [1], Elena Efremenko [1,*]

1 Faculty of Chemistry, Lomonosov Moscow State University, Lenin Hills 1/3, Moscow 119991, Russia
* Correspondence: elena_efremenko@list.ru; Tel.: +7-(495)-939-3170

Table S1. Catalytic characteristics of combinations of enzymes exhibiting lactonase activity with PAAs in reactions of hydrolysis of corresponding substrates

Enzyme	PAA	K_M, μM	V_{max}/E_0, s^{-1}	k_{eff}, $10^3 \times s^{-1} \times M^{-1}$	*p* value*
Paraoxon					
His_6-OPH	-	11.0 ± 1.2	5010 ± 210	455 ± 69	
	PLD_{50}	10.0 ± 1.9	5240 ± 360	524 ± 135	0.62
	PLE_{50}	9.0 ± 1.0	4880 ± 170	542 ± 77	0.41
Meropenem					
NDM-1	-	55 ± 16	74 ± 10	1.34 ± 0.56	
	PLD_{50}	74 ± 30	123 ± 33	1.67 ± 0.57	<0.001
	PLE_{50}	70 ± 28	114 ± 29	1.63 ± 0.55	<0.001
	$PEG_{22}PLE_{50}$	101 ± 29	165 ± 27	1.63 ± 0.72	0.088
N-(3-hydroxy-hexanoyl)-L-homoserine lactone					
AiiA	-	1.1 ± 0.2	8.0 ± 0.4	7.4 ± 1.9	
	PLD_{50}	1.5 ± 0.2	11.2 ± 0.5	7.5 ± 1.4	0.762
	PLE_{50}	2.0 ± 0.4	9.0 ± 0.4	4.5 ± 1.1	0.024

Note: One-way analysis of variance (ANOVA) test followed by Holm-Sidak method was used for pairwise multiple comparisons. A value of $p<0.05$ was considered as statistically significant.

Table S2. Catalytic characteristics of combinations of enzymes degrading fungal cell-wall components with PAAs in reactions of hydrolysis of corresponding substrates

Enzyme	PAA	K_M, g×L^{-1}	V_{max}/E_0, s^{-1}	k_{eff} ×10^3, L×s^{-1}×g^{-1}	*p* value*
Chitin azure					
ChiC	-	5.8±0.9	0.7±0.04	121±26	
	PLD_{10}	6.4±1.5	0.48±0.02	75±21	0.004
	PLE_{10}	7.9±0.8	0.51±0.03	65±11	0.023
	PLD_{50}	4.2±0.3	0.41±0.11	98±43	0.025
	PLE_{50}	6.8±0.5	0.69±0.04	101±5	0.241
	$PEG_{113}PLD_{10}$	5.9±1.3	0.54±0.09	92±35	0.031
	$PEG_{113}PLE_{10}$	6.7±0.7	0.62±0.03	93±14	0.056
	$PLE_{50}PEGPLE_{50}$	6.5±0.6	0.47±0.07	62±17	0.008
4-Methylumbelliferyl β-DN,N',N''-triacetylchitotrioside					
EGlu		(19±1) ×10^{-2}	(0.93±0.17) ×10^{-3}	4.9±1.2	
	PLD_{10}	(25±2) ×10^{-2}	(0.83±0.08) ×10^{-3}	3.3±0.6	0.044
	PLE_{10}	(32±2) ×10^{-2}	(0.78±0.11) ×10^{-3}	2.4±0.5	0.025
	PLD_{50}	(15±3) ×10^{-2}	(0.58±0.06) ×10^{-3}	3.9±1.8	0.044
	PLE_{50}	(23±7) ×10^{-2}	(0.93±0.04) ×10^{-3}	4.1±0.9	0.044
	$PEG_{113}PLD_{10}$	(22±4) ×10^{-2}	(0.81±0.11) ×10^{-3}	3.7±1.2	0.25
	$PEG_{113}PLE_{10}$	(20±3) ×10^{-2}	(0.66±0.17) ×10^{-3}	3.3±1.5	0.012
	$PLE_{50}PEGPLE_{50}$	(20±3) ×10^{-2}	(0.75±0.08) ×10^{-3}	3.8±1.1	0.003

Note: One-way analysis of variance (ANOVA) test followed by Holm-Sidak method was used for pairwise multiple comparisons. A value of $p<0.05$ was considered as statistically significant.

Table S3. Pairwise comparisons of the residual enzymatic activity of lactone-hydrolyzing enzymes alone or in combinations with PAAs when studying thermal inactivation of their enzymatic activity as a function of temperature of the medium after 15 min exposure.

Temperature, °C	Enzyme/PAA combination	*vs.* Enzyme/PLD_{50}	*vs.* Enzyme/PLE_{50}
AiiA			
37	AiiA	p = 0.018	p = 0.010
	AiiA/ PLD_{50}		n.s
50	AiiA	p = 0.001	p < 0.001
	AiiA/ PLD_{50}		p < 0.001
65	AiiA	p < 0.001	p < 0.001
	AiiA/ PLD_{50}		p < 0.001
His_6-OPH			
37	His_6-OPH	p < 0.001	p < 0.001
	His_6-OPH+ PLD_{50}		p < 0.001
50	His_6-OPH	p = 0.010	p < 0.001
	His_6-OPH/ PLD_{50}		p < 0.001
65	His_6-OPH	p < 0.001	p < 0.001
	His_6-OPH/ PLD_{50}		p < 0.001
NDM-1			
37	NDM-1	p < 0.001	p < 0.001
	NDM-1/ PLD_{50}		p = 0.002
50	NDM-1	p < 0.001	p < 0.001
	NDM-1/ PLD_{50}		p < 0.001
65	NDM-1	p = 0.004	p = 0.005
	NDM-1/ PLD_{50}		p = 0.004

Table S4. Pairwise comparisons of the residual enzymatic activity of AiiA alone and in combinations with PAAs when studying thermal inactivation of its enzymatic activity as a function of temperature of the medium after 48 h exposure at 8°C, 25°C and 37°C.

Temperature, °C	Time, h	Enzyme/PAA combination	*vs.* Enzyme / PLD_{50}	*vs.* Enzyme / PLE_{50}
AiiA				
8	2	AiiA	$p < 0.001$	n. s.
		AiiA / PLD_{50}		$p = 0.002$
	4	AiiA	$p = 0.003$	$p = 0.132$
		AiiA / PLD_{50}		$p < 0.001$
	6	AiiA	$p < 0.001$	$p = 0.025$
		AiiA / PLD_{50}		n.s
	12	AiiA	$p = 0.002$	$p = 0.029$
		AiiA / PLD_{50}		$p = 0.027$
	24	AiiA	$p = 0.005$	$p = 0.006$
		AiiA / PLD_{50}		$p = 0.003$
	48	AiiA	$p = 0.046$	n.s
		AiiA / PLD_{50}		$p = 0.102$
25	2	AiiA	$p < 0.001$	$p = 0.003$
		AiiA / PLD_{50}		$p < 0.001$
	4	AiiA	$p < 0.001$	n.s
		AiiA / PLD_{50}		$p < 0.001$
	6	AiiA	$p < 0.001$	n.s
		AiiA / PLD_{50}		$p < 0.001$
	12	AiiA	n.s	n.s
		AiiA / PLD_{50}		$p = 0.041$
	24	AiiA	$p < 0.001$	n.s
		AiiA / PLD_{50}		$p < 0.001$
	48	AiiA	$p < 0.001$	$p = 0.003$
		AiiA / PLD_{50}		$p = 0.009$
37	2	AiiA	$p < 0.001$	$p < 0.001$
		AiiA / PLD_{50}		$p < 0.001$
	4	AiiA	$p < 0.001$	$p < 0.001$
		AiiA / PLD_{50}		$p < 0.001$
	6	AiiA	$p < 0.001$	$p < 0.001$
		AiiA / PLD_{50}		$p = 0.032$
	12	AiiA	$p < 0.001$	$p < 0.001$
		AiiA / PLD_{50}		$p < 0.001$
	24	AiiA	$p < 0.001$	n.s
		AiiA / PLD_{50}		$p < 0.001$
	48	AiiA	$p < 0.001$	n.s
		AiiA / PLD_{50}		$p < 0.001$

Table S5. Pairwise comparisons of the residual enzymatic activity of His_6-OPH alone and in combinations with PAAs when studying thermal inactivation of its enzymatic activity as a function of temperature of the medium after 48 h exposure at 8°C, 25°C and 37°C.

Temperature, °C	Time, h	Enzyme/PAA combination	*vs.* Enzyme / PLD_{50}	*vs.* Enzyme / PLE_{50}
8	2	His_6-OPH	$p < 0.001$	$p < 0.001$
		His_6-OPH / PLD_{50}		$p < 0.001$
	4	His_6-OPH	$p < 0.001$	$p < 0.001$
		His_6-OPH / PLD_{50}		$p < 0.001$
	6	His_6-OPH	$p < 0.001$	$p < 0.001$
		His6-OPH / PLD_{50}		$p < 0.001$
	24	His_6-OPH	$p < 0.001$	$p < 0.001$
		His_6-OPH / PLD_{50}		$p < 0.001$
	48	His_6-OPH	$p < 0.001$	$p < 0.001$
		His_6-OPH / PLD_{50}		$p < 0.001$
25	2	His_6-OPH	$p < 0.001$	$p < 0.001$
		His_6-OPH / PLD_{50}		$p < 0.001$
	4	His_6-OPH	$p < 0.001$	$p < 0.001$
		His_6-OPH / PLD_{50}		$p < 0.001$
	6	His_6-OPH	$p < 0.001$	$p < 0.001$
		His_6-OPH / PLD_{50}		$p < 0.001$
	24	His_6-OPH	$p < 0.001$	$p < 0.001$
		His_6-OPH / PLD_{50}		$p < 0.001$
	48	His_6-OPH	$p < 0.001$	$p < 0.001$
		His_6-OPH / PLD_{50}		$p < 0.001$
37	2	His_6-OPH	$p = 0.001$	$p < 0.001$
		His_6-OPH / PLD_{50}		$p = 0.003$
	4	His_6-OPH	$p < 0.001$	$p < 0.001$
		His_6-OPH / PLD_{50}		n.s
	6	His_6-OPH	$p = 0.005$	$p < 0.001$
		His_6-OPH / PLD_{50}		$p < 0.001$
	24	His_6-OPH	$p < 0.001$	$p < 0.001$
		His_6-OPH / PLD_{50}		$p = 0.002$
	48	His_6-OPH	$p < 0.001$	$p < 0.001$
		His_6-OPH / PLD_{50}		$p < 0.001$

Table S6. Pairwise comparisons of the residual enzymatic activity of NDM-1 alone and in combinations with PAAs when studying thermal inactivation of its enzymatic activity as a function of temperature of the medium after 48 h exposure at 8°C, 25°C and 37°C.

Temperature, °C	Time, h	Enzyme/PAA combination	*vs.* Enzyme / PLD_{50}	*vs.* Enzyme / PLE_{50}
8	2	NDM-1	$p < 0.001$	$p < 0.001$
		NDM-1 / PLD_{50}		$p < 0.001$
	4	NDM-1	$p = 0.005$	$p < 0.001$
		NDM-1 / PLD_{50}		$p < 0.001$
	6	NDM-1	$p < 0.001$	$p = 0.004$
		NDM-1 / PLD_{50}		$p < 0.001$
	24	NDM-1	$p < 0.001$	$p = 0.430$
		NDM-1 / PLD_{50}		$p < 0.001$
	48	NDM-1	$p < 0.001$	$p < 0.001$
		NDM-1 / PLD_{50}		$p < 0.001$
25	2	NDM-1	$p < 0.001$	$p < 0.001$
		NDM-1 / PLD_{50}		$p < 0.001$
	4	NDM-1	$p < 0.001$	$p < 0.001$
		NDM-1 / PLD_{50}		$p < 0.001$
	6	NDM-1	$p < 0.001$	$p < 0.001$
		NDM-1 / PLD_{50}		$p < 0.001$
	24	NDM-1	$p < 0.001$	$p < 0.001$
		NDM-1 / PLD_{50}		$p < 0.001$
	48	NDM-1	$p < 0.001$	$p < 0.001$
		NDM-1 / PLD_{50}		$p < 0.001$
37	2	NDM-1	$p = 0.003$	$p = 0.002$
		NDM-1 / PLD_{50}		$p < 0.001$
	4	NDM-1	$p < 0.001$	$p < 0.001$
		NDM-1 / PLD_{50}		$p < 0.001$
	6	NDM-1	$p < 0.001$	$p < 0.001$
		NDM-1 / PLD_{50}		$p < 0.001$
	24	NDM-1	$p < 0.001$	$p < 0.001$
		NDM-1 / PLD_{50}		$p < 0.001$
	48	NDM-1	$p < 0.001$	$p < 0.001$
		NDM-1 / PLD_{50}		$p < 0.001$

Table S7. Nanoparticles tracking analysis of particle size of enzyme-PAA combinations

Enzyme	PAA	Median, nm	Concentration × 10^8, particles/mL
His_6-OPH	-	7 ± 2	25 ± 2
	PLD_{50}	43 ± 10	27 ± 2
	PLE_{50}	32 ± 6	28 ± 2
NDM-1	-	5 ± 2	50 ± 5
	PLD_{50}	39 ± 8	35 ± 4
	PLE_{50}	40 ± 9	32 ± 3
	$PEG_{22}PLE_{50}$	62 ± 13	29 ± 3
AiiA	-	4 ± 1	31 ± 4
	PLD_{50}	38 ± 9	47 ± 3
	PLE_{50}	36 ± 7	44 ± 4
ChiC	-	70±10	40±4
	PLD_{10}	75±5	35±5
	PLE_{10}	85±10	40± 5
	PLD_{50}	90±20	40±5
	PLE_{50}	87±7	35±5
	$PEG_{113}PLD_{10}$	115±10	45±5
	$PEG_{113}PLE_{10}$	105±10	40±5
	$PLE_{50}PEGPLE_{50}$	150±10	40±4
EGlu	-	60±5	40±5
	PLD_{10}	65±5	40±4
	PLE_{10}	60±8	35± 5
	PLD_{50}	80±10	40±5
	PLE_{50}	80±5	35±3
	$PEG_{113}PLD_{10}$	90±5	40±5
	$PEG_{113}PLE_{10}$	85±5	40±2
	$PLE_{50}PEGPLE_{50}$	110±5	45±10

Table S8. The area occupied by the fungicides molecules near the active site on the surface of the enzyme or on its total surface and the affinity of the fungicides molecules to the surface of enzymes.

Enzyme	Polymer	Fungicide	Area (%)*		Affinity (kcal×mol^{-1})
			Near active site	Total	
AiiA	PLD_{50}	Zineb	0.0	8.5	-6.8 ± 0.2
		Clotrimazole	22.3	9.2	-3.5 ± 0.2
	PLE_{50}	Zineb	0.0	6.3	-7.0 ± 0.1
		Clotrimazole	22.3	4.2	-3.3 ± 0.2
His_6-OPH	PLD_{50}	Zineb	12.0	3.9	-6.8 ± 0.1
		Clotrimazole	0.0	3.2	-3.5 ± 0.1
	PLE_{50}	Zineb	12.0	5.3	-6.9 ± 0.2
		Clotrimazole	12.0	4.5	-3.1 ± 0.1
NDM-1	PLD_{50}	Zineb	18.4	4.4	-6.5 ± 0.4
		Clotrimazole	0.0	2.5	-3.5 ± 0.1
	PLE_{50}	Zineb	16.5	7.8	-6.1 ± 0.3
		Clotrimazole	0.0	6.4	-3.3 ± 0.3
Bgy6	PLD_{50}	Zineb	2.7	2.8	-6.4 ± 0.2
		Clotrimazole	17.0	4.5	-3.4 ± 0.2
	PLE_{50}	Zineb	2.7	2.9	-6.8 ± 0.3
		Clotrimazole	0.0	2.4	-3.8 ± 0.1
ChiC	PLD_{50}	Zineb	16.2	3.0	-6.6 ± 0.2
		Clotrimazole	16.2	3.7	-3.6 ± 0.2
	PLE_{50}	Zineb	0.0	3.0	-6.7 ± 0.2
		Clotrimazole	81.7	5.1	-3.4 ± 0.1

Note: The value of the surface area of the active sites of enzyme and the value of the area of the total surface of enzyme are taken as 100%

Table S9. Residual intracellular ATP levels (%) in filamentous fungi and yeasts were measured after 24 h of treatment with enzymes exhibiting lactonase activity [8] and enzymes degrading fungal cell-wall components themselves (activity in the absence of AMPs and PAAs). The residual concentration of ATP in control samples with cells without the addition of antimicrobial agents was taken as 100%.

Microorganisms	AiiA	His_6-OPH	NDM-1	ChiC	Bgy6
Aspergillus niger	100 ± 1	73 ± 4	100 ± 2	100 ±2.7	24 ±2.1
Fusarium solani	0.1 ± 0.02	97 ± 3	0.2 ± 0.05	31 ±5	87 ±2.1
Trichoderma atroviride	1.5 ± 0.5	100 ± 2	1.1 ± 0.3	30 ±3	100 ±3
Rhizopus oryzae	21 ± 1	41 ± 3	20 ± 1	8 ±1	100 ±4.8
Saccharomyces cerevisiae	100 ± 2	99 ± 3	100 ± 3	26 ±1	85 ±5.8
Candida tropicalis	100 ± 3	98 ± 2	100 ± 1	88 ±1.8	15 ±2.5

Table S10. Pairwise comparisons of the residual concentrations of intracellular ATP in different filamentous fungi and yeasts in the presence of combinations of lactonases with AMPs [8].

Microorganism	Enzyme/AMP combination	*vs.* AMP	
		Polymyxin B	Colstin
Aspergillus niger	AiiA/Polymyxin B	p<0.001	
	AiiA/Colistin		p=0.033
	His_6-OPH /Polymyxin B	p<0.001	
	His_6-OPH/Colistin		p=0.013
	NDM-1/Polymyxin B	p<0.001	
	NDM-1/Colistin		p<0.001
Fusarium solani	AiiA/Polymyxin B	n.s	
	AiiA/Colistin		n.s
	His_6-OPH /Polymyxin B	n.s	
	His_6-OPH/Colistin		n.s
	NDM-1/Polymyxin B	n.s	
	NDM-1/Colistin		n.s
Trichoderma atroviride	AiiA/Polymyxin B	n.s	
	AiiA/Colistin		p<0.001
	His_6-OPH /Polymyxin B	n.s	
	His_6-OPH/Colistin		p<0.001
	NDM-1/Polymyxin B	n.s	
	NDM-1/Colistin		n.s
Rhizopus oryzae	AiiA/Polymyxin B	p=0.004	
	AiiA/Colistin		p<0.001
	His_6-OPH /Polymyxin B	p=0.025	
	His_6-OPH/Colistin		p<0.001
	NDM-1/Polymyxin B	n.s	
	NDM-1/Colistin		n.s
Saccharomyces cerevisiae	AiiA/Polymyxin B	p<0.001	
	AiiA/Colistin		p=0.006
	His_6-OPH /Polymyxin B	p<0.001	
	His_6-OPH/Colistin		p=0.003
	NDM-1/Polymyxin B	n.s	
	NDM-1/Colistin		n.s
Candida tropicalis	AiiA/Polymyxin B	p<0.001	
	AiiA/Colistin		p=0.002
	His_6-OPH /Polymyxin B	p<0.001	
	His_6-OPH/Colistin		p=0.002
	NDM-1/Polymyxin B	n.s	
	NDM-1/Colistin		n.s

Table S11. Pairwise comparisons of the residual concentrations of intracellular ATP in different filamentous fungi and yeasts in the presence of combinations of lactonases with PAAs, supplemented with Clotrimazole.

Microorganism	Clotrimazole combined with	*vs.* Clotrimazole
Aspergillus niger	AiiA/PLD$_{50}$	$p<0.001$
	AiiA/PLE$_{50}$	$p<0.001$
	His$_6$-OPH/PLD$_{50}$	$p<0.001$
	His$_6$-OPH/PLE$_{50}$	$p<0.001$
	NDM-1/PLD$_{50}$	$p<0.001$
	NDM-1/PLE$_{50}$	$p<0.001$
Fusarium solani	AiiA/PLD$_{50}$	$p<0.001$
	AiiA/PLE$_{50}$	$p<0.001$
	His$_6$-OPH/PLD$_{50}$	$p<0.001$
	His$_6$-OPH/PLE$_{50}$	$p<0.001$
	NDM-1/PLD$_{50}$	$p<0.001$
	NDM-1/PLE$_{50}$	$p<0.001$
Trichoderma atroviride	AiiA/PLD$_{50}$	$p=0.005$
	AiiA/PLE$_{50}$	$p=0.006$
	His$_6$-OPH/PLD$_{50}$	$p<0.001$
	His$_6$-OPH/PLE$_{50}$	$p<0.001$
	NDM-1/PLD$_{50}$	n.s.
	NDM-1/PLE$_{50}$	$p=0.002$
Rhizopus oryzae	AiiA/PLD$_{50}$	$p=0.017$
	AiiA/PLE$_{50}$	$p=0.038$
	His$_6$-OPH/PLD$_{50}$	$p<0.001$
	His$_6$-OPH/PLE$_{50}$	$p<0.001$
	NDM-1/PLD$_{50}$	$p=0.006$
	NDM-1/PLE$_{50}$	$p=0.007$
Saccharomyces cerevisiae	AiiA/PLD$_{50}$	$p=0.001$
	AiiA/PLE$_{50}$	$p<0.001$
	His$_6$-OPH/PLD$_{50}$	$p<0.001$
	His$_6$-OPH/PLE$_{50}$	$p<0.001$
	NDM-1/PLD$_{50}$	$p<0.001$
	NDM-1/PLE$_{50}$	$p=0.008$
Candida tropicalis	AiiA/PLD$_{50}$	$p<0.001$
	AiiA/PLE$_{50}$	$p=0.003$
	His$_6$-OPH/PLD$_{50}$	n.s.
	His$_6$-OPH/PLE$_{50}$	$p<0.001$
	NDM-1/PLD$_{50}$	$p<0.001$
	NDM-1/PLE$_{50}$	$p<0.001$

Table S12. Pairwise comparisons of the residual concentrations of intracellular ATP in different filamentous fungi and yeasts in the presence of combinations of cell-wall degrading enzymes with AMPs.

Microorganism	Enzyme/AMP	*vs.* AMP	
		Polymyxin B	Colstin
Aspergillus niger	ChiC/Polymyxin B	$p < 0.001$	
	ChiC/Colistin		$p = 0.002$
	Bgy6/Polymyxin B	$p < 0.001$	
	Bgy6/Colistin		$p < 0.001$
Fusarium solani	ChiC/Polymyxin B	$p = 0.001$	
	ChiC/Colistin		$p < 0.001$
	Bgy6/Polymyxin B	n.s.	
	Bgy6/Colistin		n.s.
Trichoderma atroviride	ChiC/Polymyxin B	$p < 0.001$	
	ChiC/Colistin		$p = 0.033$
	Bgy6/Polymyxin B	n.s.	
	Bgy6/Colistin		$p = 0.035$
Rhizopus oryzae	ChiC/Polymyxin B	$p < 0.001$	
	ChiC/Colistin		$p = 0.002$
	Bgy6/Polymyxin B	$p < 0.001$	
	Bgy6/Colistin		$p = 0.002$
Saccharomyces cerevisiae	ChiC/Polymyxin B	$p < 0.001$	
	ChiC/Colistin		$p < 0.001$
	Bgy6/Polymyxin B	n.s.	
	Bgy6/Colistin		$p < 0.001$
Candida tropicalis	ChiC/Polymyxin B	$p < 0.001$	
	ChiC/Colistin		$p < 0.001$
	Bgy6/Polymyxin B	n.s.	
	Bgy6/Colistin		$p < 0.001$

Table S13. Pairwise comparisons of the residual concentrations of intracellular ATP in different filamentous fungi and yeasts in the presence of combinations of cell-wall degrading enzymes with PAAs supplemented with Clotrimazole.

Microorganism	Clotrimazole combined with	*vs.* Clotrimazole
Aspergillus niger	ChiC/PLD$_{50}$	n.s.
	ChiC/PLE$_{50}$	$p<0.001$
	Bgy6/PLD$_{50}$	$p<0.001$
	Bgy6/PLE$_{50}$	$p<0.001$
Fusarium solani	ChiC/PLD$_{50}$	$p<0.001$
	ChiC/PLE$_{50}$	$p<0.001$
	Bgy6/PLD$_{50}$	$p<0.001$
	Bgy6/PLE$_{50}$	$p=0.001$
Trichoderma atroviride	ChiC/PLD$_{50}$	$p=0.023$
	ChiC/PLE$_{50}$	$p<0.001$
	Bgy6/PLD$_{50}$	$p<0.001$
	Bgy6/PLE$_{50}$	$p=0.023$
Rhizopus oryzae	ChiC/PLD$_{50}$	$p=0.006$
	ChiC/PLE$_{50}$	$p<0.001$
	Bgy6/PLD$_{50}$	$p<0.001$
	Bgy6/PLE$_{50}$	$p=0.008$
Saccharomyces cerevisiae	ChiC/PLD$_{50}$	$p<0.001$
	ChiC/PLE$_{50}$	$p<0.001$
	Bgy6/PLD$_{50}$	$p<0.001$
	Bgy6/PLE$_{50}$	$p<0.001$
Candida tropicalis	ChiC/PLD$_{50}$	n.s.
	ChiC/PLE$_{50}$	$p=0.017$
	Bgy6/PLD$_{50}$	$p=0.014$
	Bgy6/PLE$_{50}$	$p<0.001$

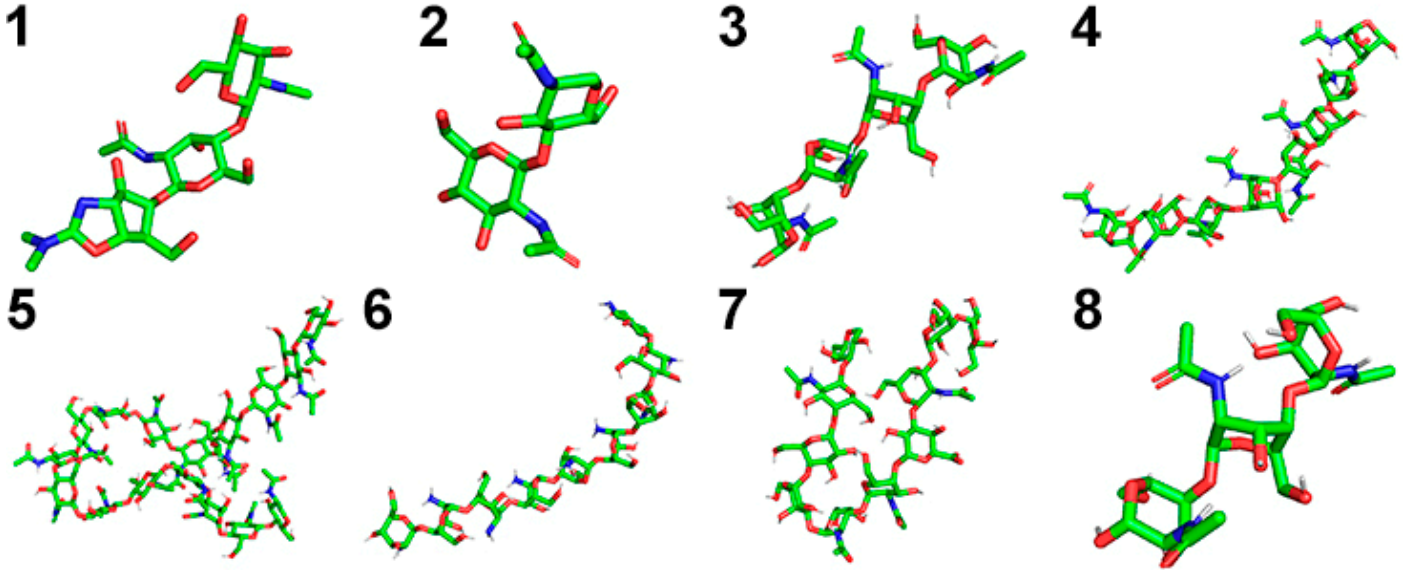


Figure S1. 3D structure of model molecules of fungal cell wall components: Allosamidin (1), Chitin dimer (2), Chitin tetramer (3), Chitin octamer (4), Chitin octadecamer (5), Chitosan (6), Galactosaminogalactan (7), Triacetylchitotriose (8).

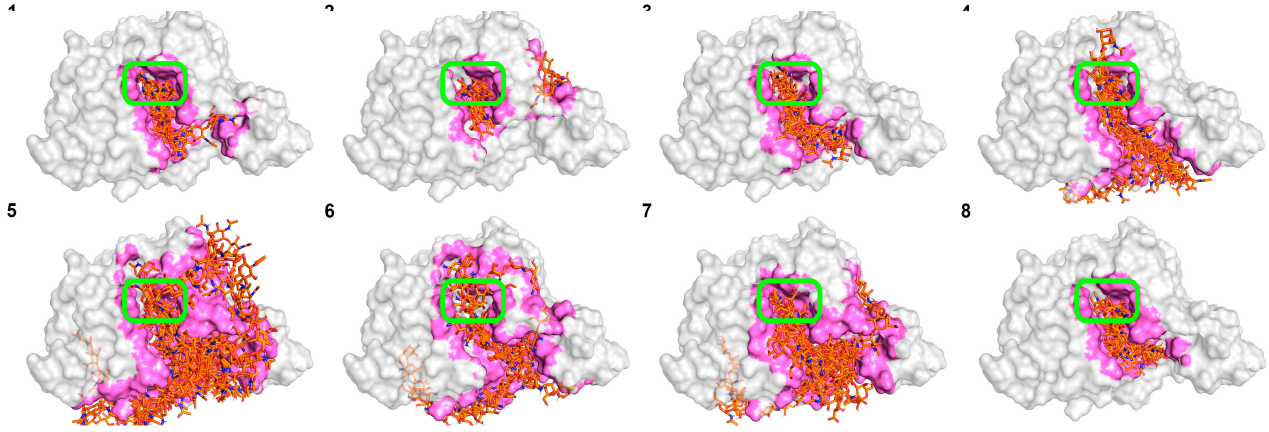


Figure S2. The localization of molecules of fungal cell wall components (Allosamidin (1), Chitin dimer (2), Chitin tetramer (3), Chitin octamer (4), Chitin octadecamer (5), Chitosan (6), Galactosaminogalactan (7), Triacetylchitotriose (8)) on the surface of fungal cell wall degrading enzyme Bgy6. The molecular surface of the enzymes is colored gray. The molecules of fungal cell wall components are shown as sticks. Atoms of the enzyme situated within 4 Å of substrate molecules, along with the corresponding molecular surface regions, are depicted in purple. The entrances to the enzymatic active sites are marked with green boxes.

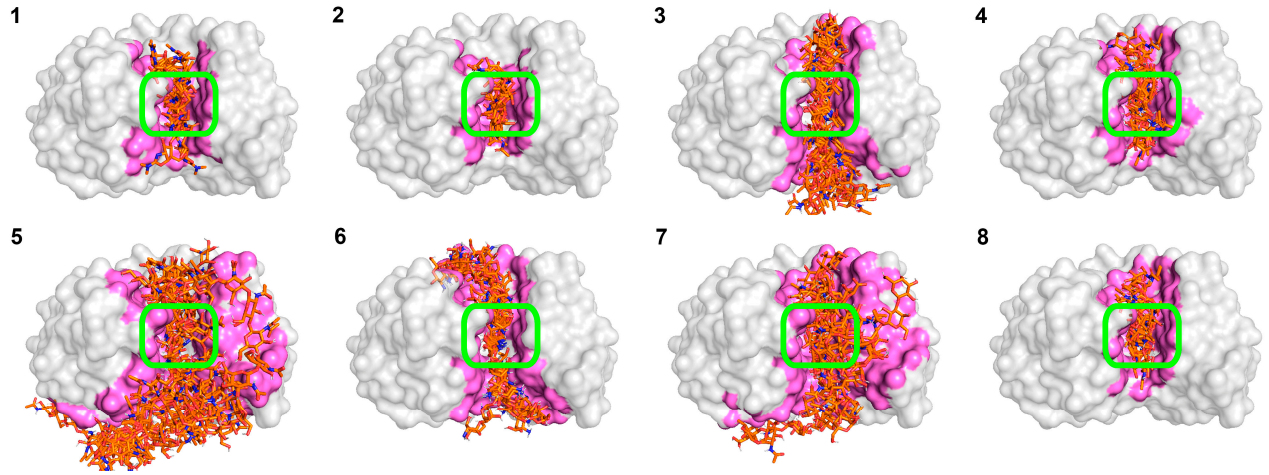


Figure S3. The localization of molecules of fungal cell wall components (Allosamidin (1), Chitin dimer (2), Chitin tetramer (3), Chitin octamer (4), Chitin octadecamer (5), Chitosan (6), Galactosaminogalactan (7), Triacetylchitotriose (8)) on the surface of fungal cell wall degrading enzyme ChiC. The molecular surface of the enzymes is colored gray. The molecules of fungal cell wall components are shown as sticks. The atoms located within 4 Å of any substrate atom and the corresponding molecular surface of enzymes is depicted in purple. The entrances to the enzymatic active sites are marked with green boxes.

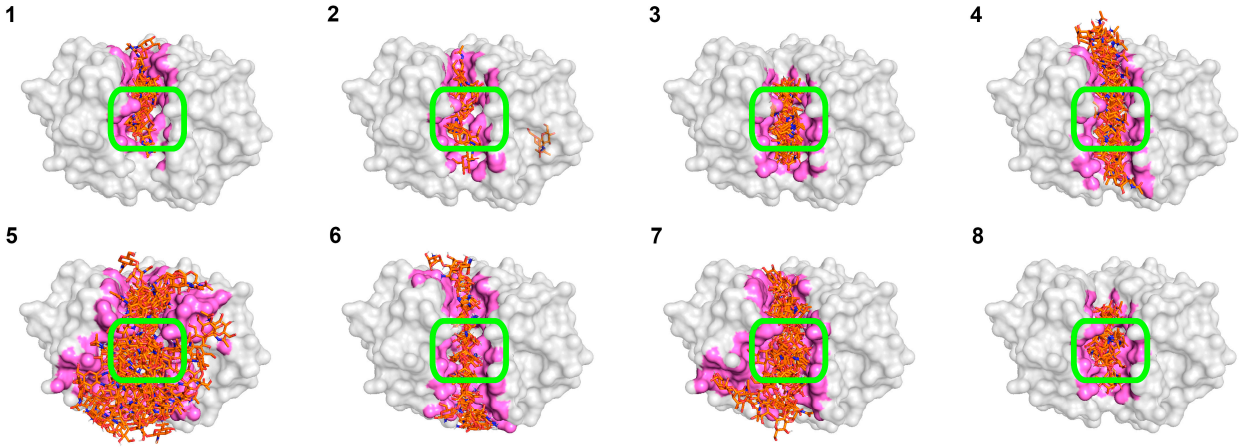


Figure S4. The localization of molecules of fungal cell wall components (Allosamidin (1), Chitin dimer (2), Chitin tetramer (3), Chitin octamer (4), Chitin octadecamer (5), Chitosan (6), Galactosaminogalactan (7), Triacetylchitotriose (8)) on the surface of fungal cell wall degrading enzyme Ega3. The molecular surface of the enzymes is depicted in gray. The molecules of fungal cell wall components are shown as sticks. Atoms of the enzyme situated within 4 Å of substrate molecules, together with the corresponding molecular surface regions, are depicted in purple. The entrances to the enzymatic active sites are marked with green boxes.

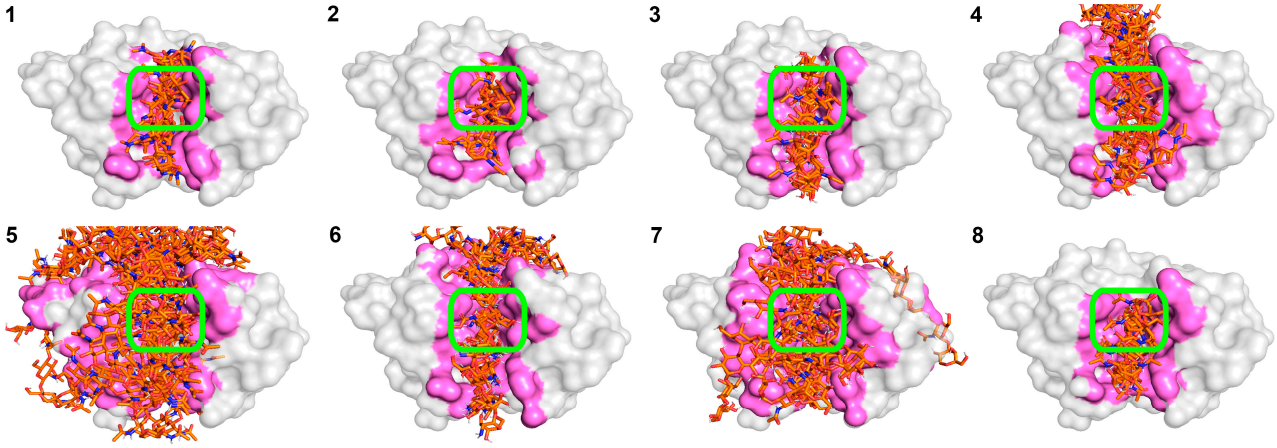


Figure S5. The localization of molecules of fungal cell wall components (Allosamidin (1), Chitin dimer (2), Chitin tetramer (3), Chitin octamer (4), Chitin octadecamer (5), Chitosan (6), Galactosaminogalactan (7), Triacetylchitotriose (8)) on the surface of fungal cell wall degrading enzyme Lysozyme. The enzymes' molecular surfaces are rendered in gray, and fungal cell wall component molecules are represented as sticks. Atoms situated within 4 Å of substrate molecules, along with the corresponding molecular surface regions, are depicted in purple. Active site entrances are marked with green boxes.

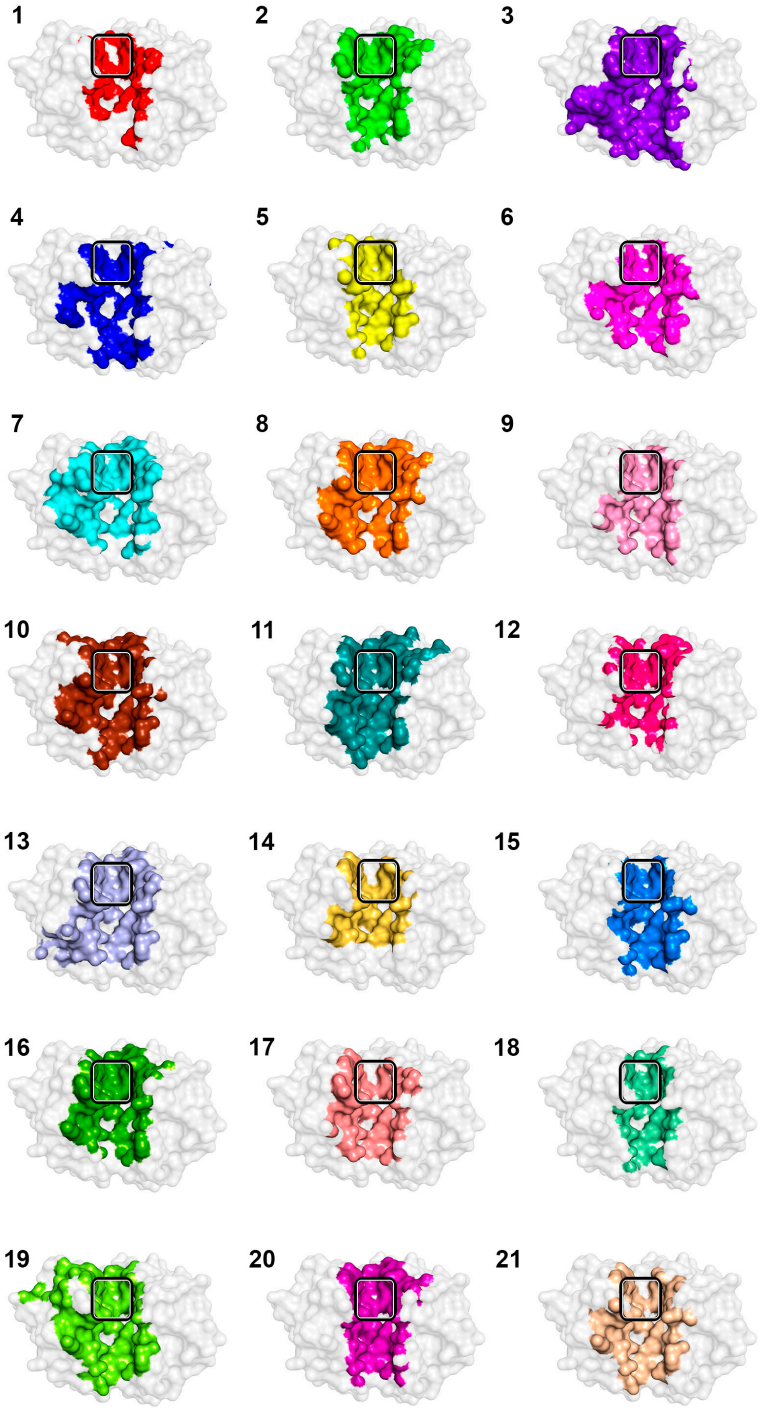


Figure S6. The localization of AMP molecules (Aculeacin A (1), Bacitracin (2), BMAP-18 (3), Bralicidin (4), Caspofungin (5), Colistin (6), Fengycin (7), Indolicidin (8), Iturin A (9), KK14 (10), Leg2 (11), hLF 1-11 (12), Lfampin B (13), PAF26 (14), PepGAT (15), PepKAA (16), Polymyxin B (17), RcAlb-PepII (18), TC3 (19), Temporin A (20), Temporin G (21)) on the surface of fungal cell wall degrading enzyme Ega3. The enzyme's molecular surface is shown in gray. Enzyme atoms within 4 Å of AMP molecules, together with the associated molecular surface, are color-coded individually for each AMP. Active site entrances are indicated by black boxes.

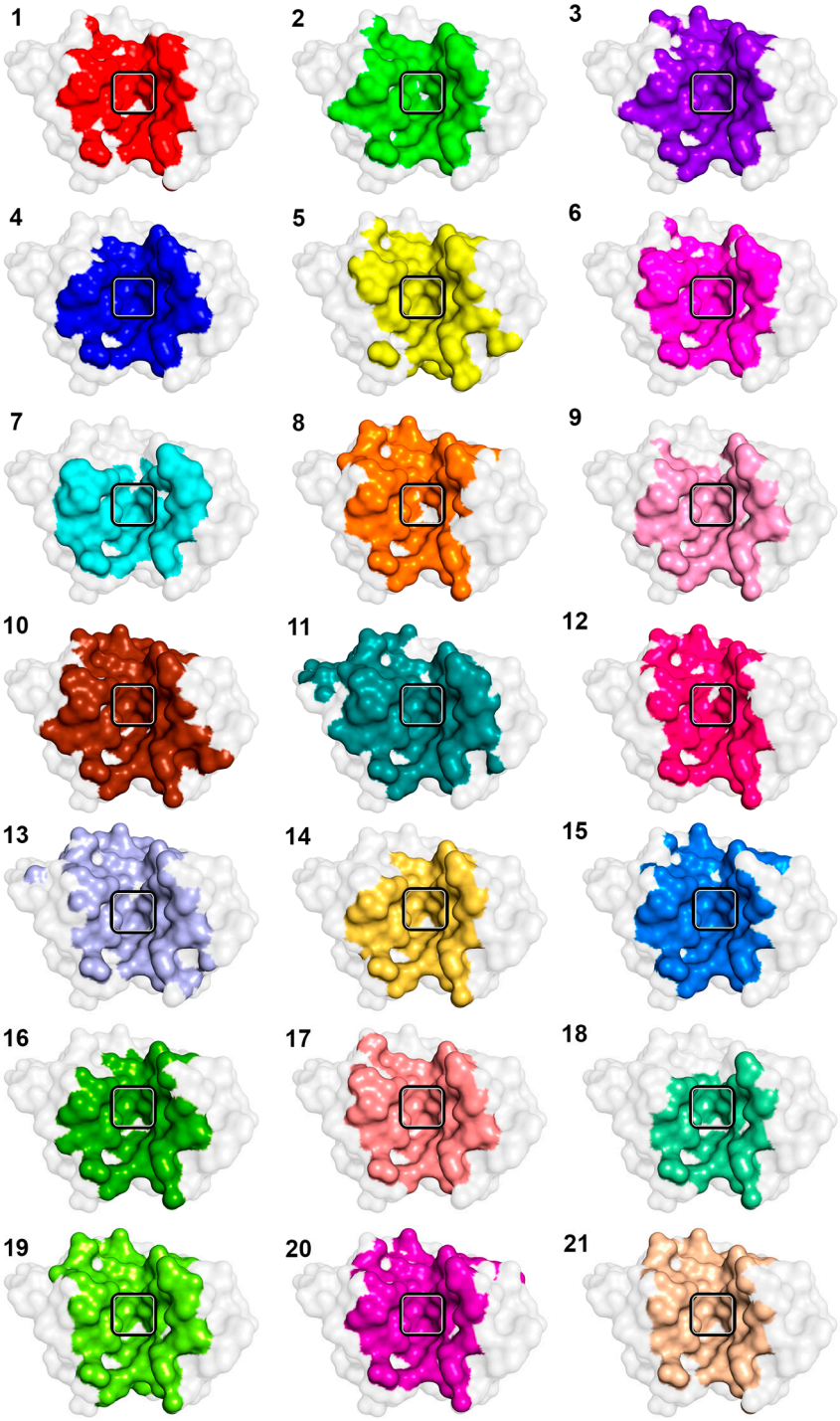


Figure S7. The localization of AMP molecules (Aculeacin A (1), Bacitracin (2), BMAP-18 (3), Bralicidin (4), Caspofungin (5), Colistin (6), Fengycin (7), Indolicidin (8), Iturin A (9), KK14 (10), Leg2 (11), hLF 1-11 (12), Lfampin B (13), PAF26 (14), PepGAT (15), PepKAA (16), Polymyxin B (17), RcAlb-PepII (18), TC3 (19), Temporin A (20), Temporin G (21)) on the surface of fungal cell wall degrading enzyme Lysozyme. The molecular surface of the enzyme is depicted in gray. Atoms located within 4 Å of AMP molecules, together with the corresponding molecular surface regions, are highlighted in distinct colors for each AMP. The entrances to the enzymatic active sites are marked with black boxes.

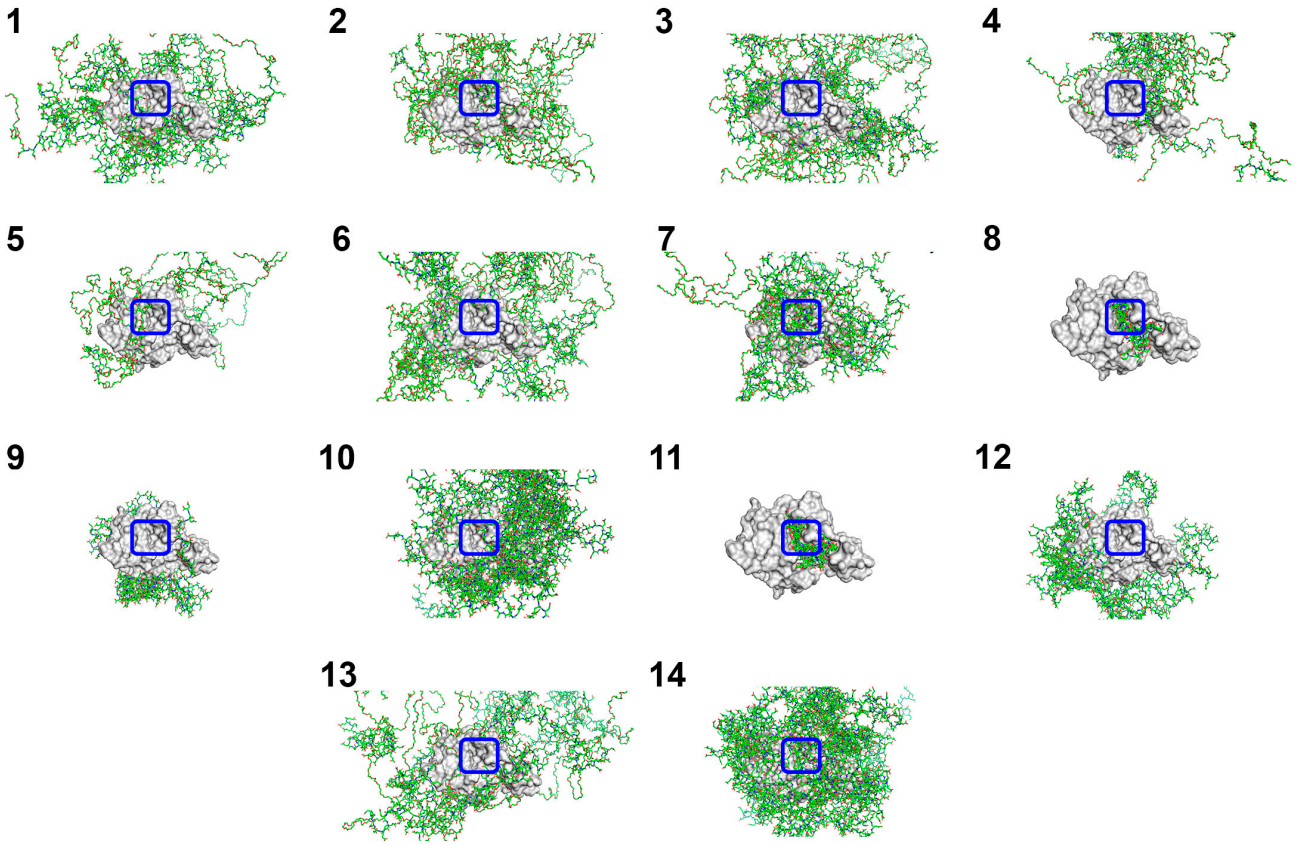


Figure S8. The localization of PAAs molecules ($PEG_{22}PLE_{50}$ (1), $PEG_{113}PLD_{10}$ (2), $PEG_{113}PLD_{50}$ (3), $PEG_{113}PLD_{100}$ (4), $PEG_{113}PLE_{10}$ (5), $PEG_{113}PLE_{50}$ (6), $PEG_{113}PLE_{100}$ (7), PLD_{10} (8), PLD_{50} (9), PLD_{100} (10), PLE_{10} (11), PLE_{50} (12), $PLE_{50}PEG_{113}PLE_{50}$ (13), PLE_{100} (14)) on the surface of Bgy6. The molecular surface of the enzyme is depicted in gray. Molecules of PAAs are shown as green sticks. The entrances to the active sites of enzymes are highlighted with blue boxes.

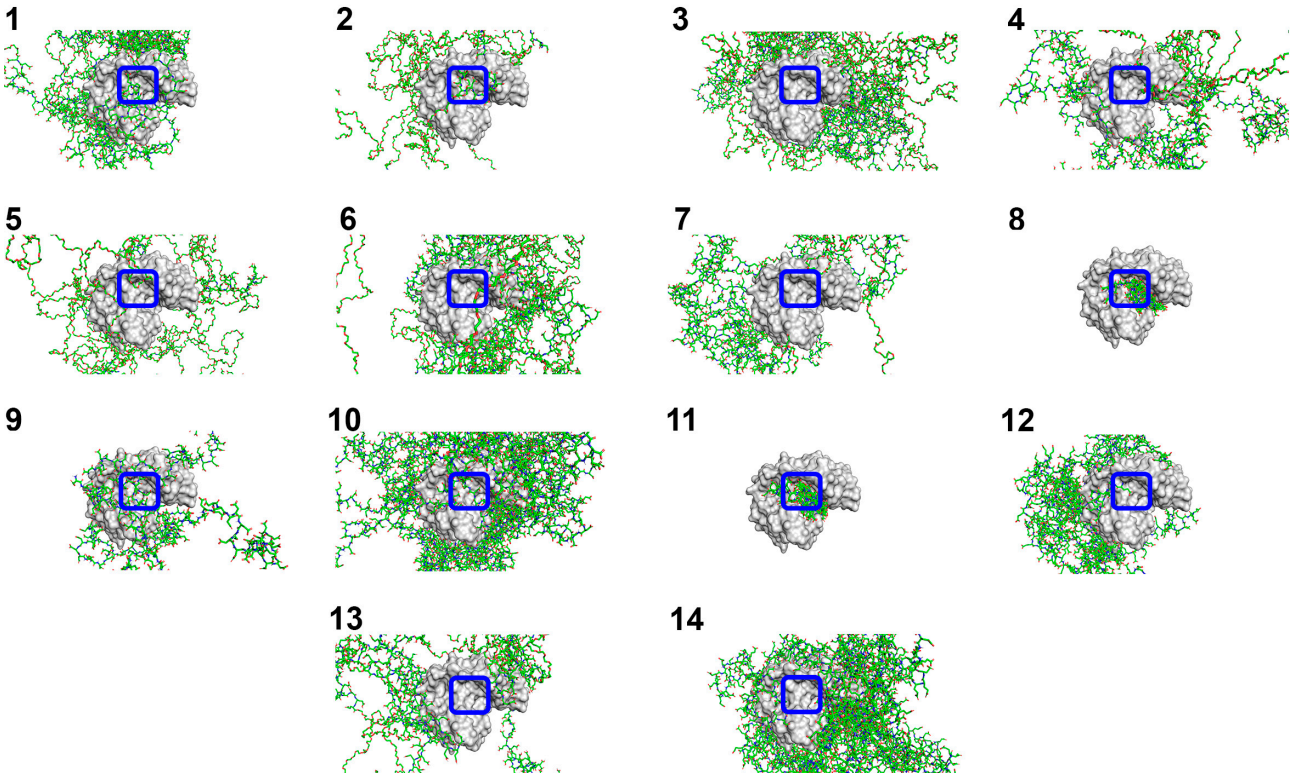


Figure S9. The localization of PAAs molecules ($PEG_{22}PLE_{50}$ (1), $PEG_{113}PLD_{10}$ (2), $PEG_{113}PLD_{50}$ (3), $PEG_{113}PLD_{100}$ (4), $PEG_{113}PLE_{10}$ (5), $PEG_{113}PLE_{50}$ (6), $PEG_{113}PLE_{100}$ (7), PLD_{10} (8), PLD_{50} (9), PLD_{100} (10), PLE_{10} (11), PLE_{50} (12), $PLE_{50}PEG_{113}PLE_{50}$ (13), PLE_{100} (14)) on the surface of ChiC. The molecular surface of the enzyme is depicted in gray. Molecules of PAAs are shown as green sticks. The entrances to the active sites of enzymes are highlighted with blue boxes.

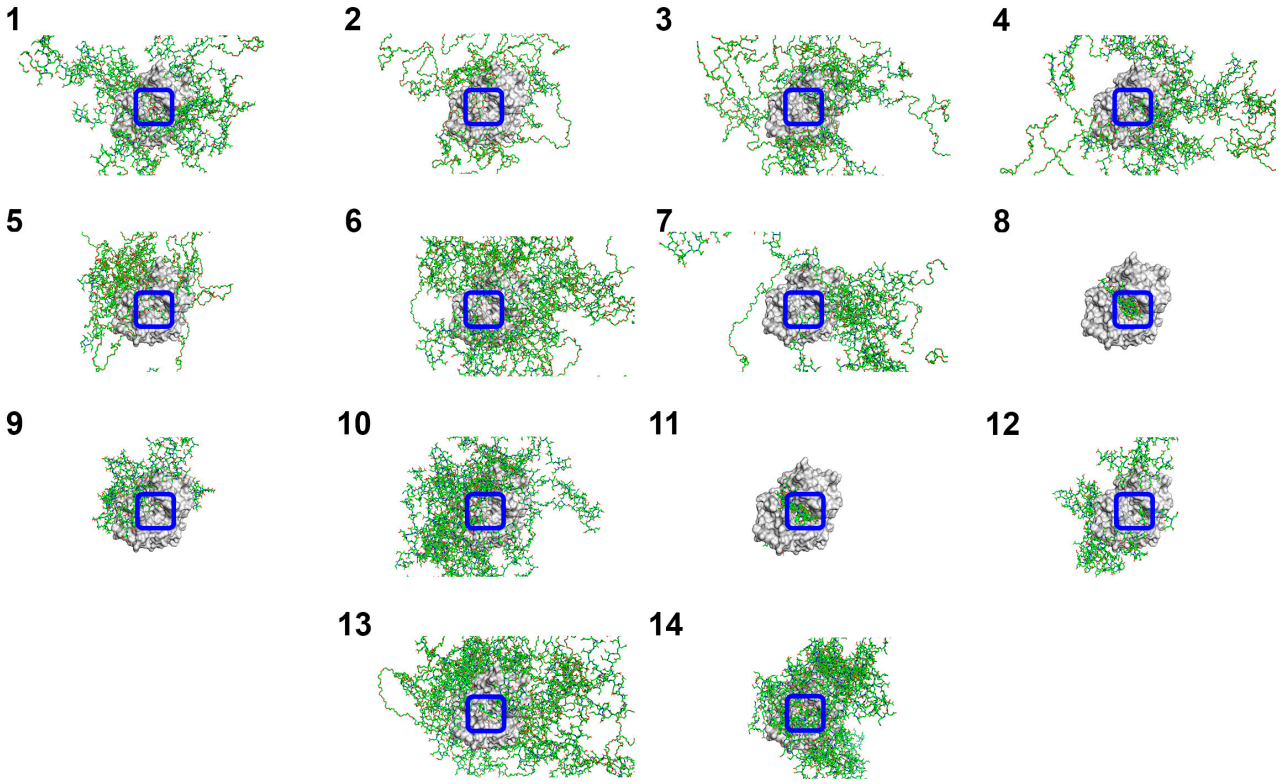


Figure S10. The localization of PAAs molecules ($PEG_{22}PLE_{50}$ (1), $PEG_{113}PLD_{10}$ (2), $PEG_{113}PLD_{50}$ (3), $PEG_{113}PLD_{100}$ (4), $PEG_{113}PLE_{10}$ (5), $PEG_{113}PLE_{50}$ (6), $PEG_{113}PLE_{100}$ (7), PLD_{10} (8), PLD_{50} (9), PLD_{100} (10), PLE_{10} (11), PLE_{50} (12), $PLE_{50}PEG_{113}PLE_{50}$ (13), PLE_{100} (14)) on the surface of Ega3. The molecular surface of the enzyme is depicted in gray. Molecules of PAAs are shown as green sticks. The entrances to the active sites of enzymes are highlighted with blue boxes.

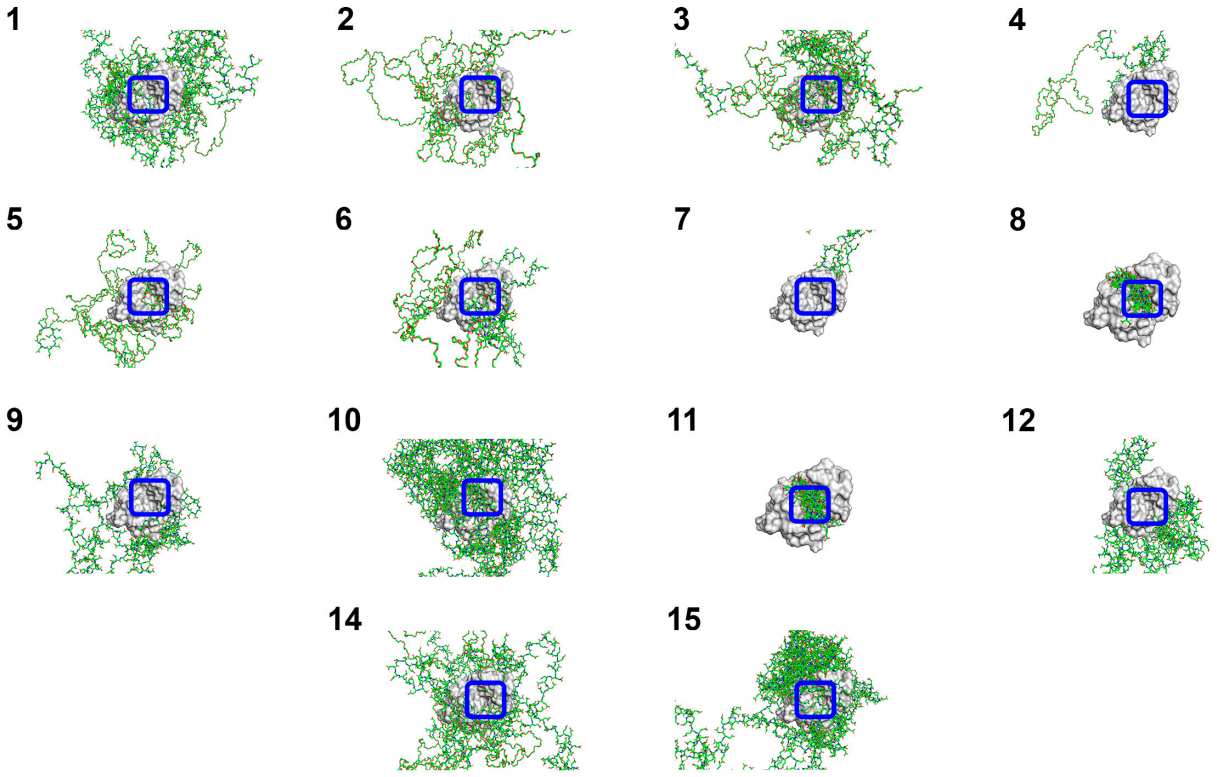


Figure S11. The localization of PAAs molecules ($PEG_{22}PLE_{50}$ (1), $PEG_{113}PLD_{10}$ (2), $PEG_{113}PLD_{50}$ (3), $PEG_{113}PLD_{100}$ (4), $PEG_{113}PLE_{10}$ (5), $PEG_{113}PLE_{50}$ (6), $PEG_{113}PLE_{100}$ (7), PLD_{10} (8), PLD_{50} (9), PLD_{100} (10), PLE_{10} (11), PLE_{50} (12), $PLE_{50}PEG_{113}PLE_{50}$ (13), PLE_{100} (14)) on the surface of Lysozyme. The molecular surface of the enzyme is depicted in gray. Molecules of PAAs are shown as green sticks. The entrances to the enzymatic active sites are marked with blue boxes.

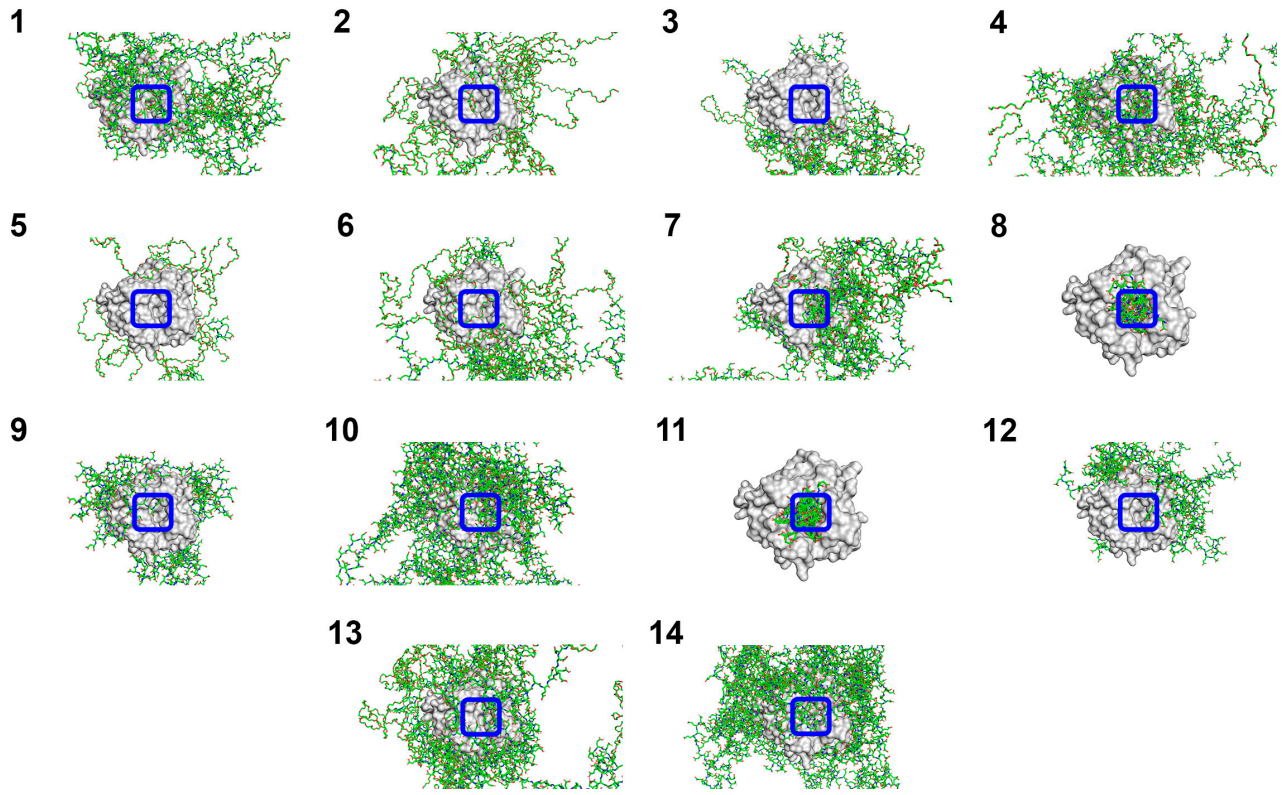


Figure S12. The localization of PAAs molecules ($PEG_{22}PLE_{50}$ (1), $PEG_{113}PLD_{10}$ (2), $PEG_{113}PLD_{50}$ (3), $PEG_{113}PLD_{100}$ (4), $PEG_{113}PLE_{10}$ (5), $PEG_{113}PLE_{50}$ (6), $PEG_{113}PLE_{100}$ (7), PLD_{10} (8), PLD_{50} (9), PLD_{100} (10), PLE_{10} (11), PLE_{50} (12), $PLE_{50}PEG_{113}PLE_{50}$ (13), PLE_{100} (14)) on the surface of AiiA. The molecular surface of the enzyme is colored gray. Molecules of PAAs are shown as green sticks. The entrances to the active sites of enzymes are highlighted with blue boxes.

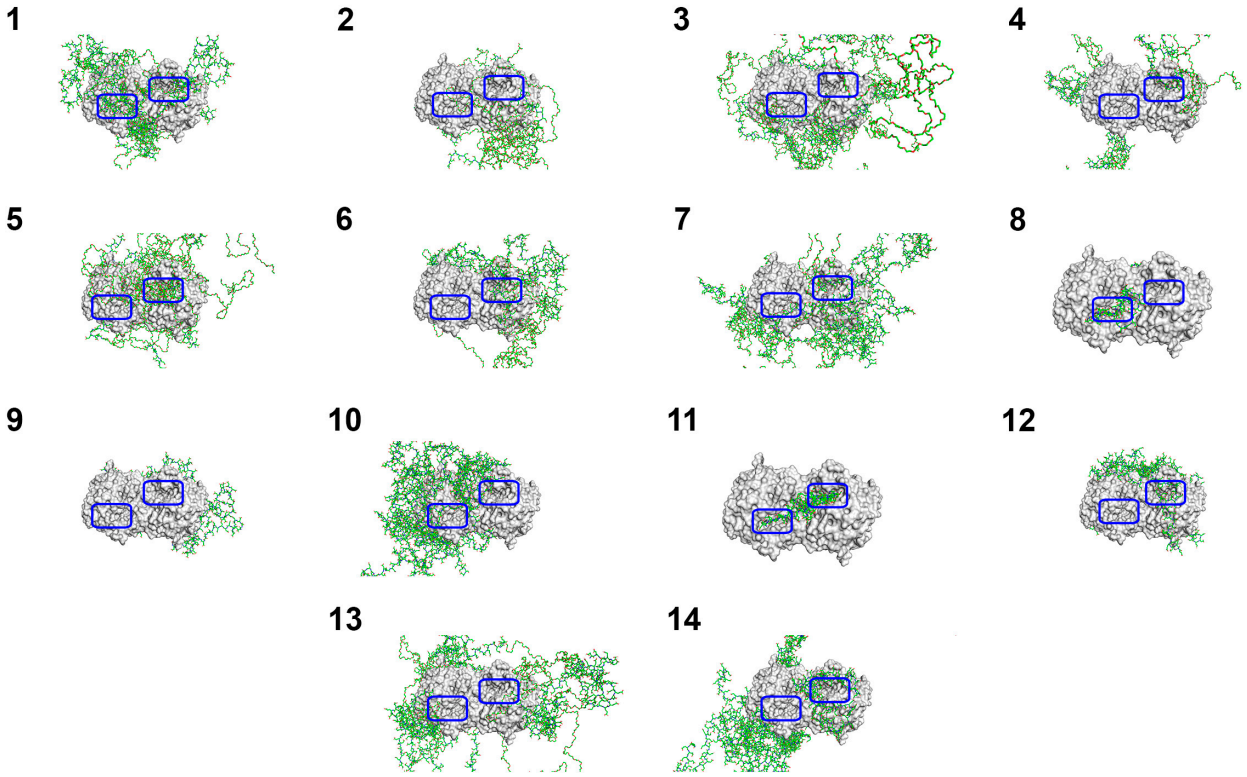


Figure S13. The localization of PAAs molecules ($PEG_{22}PLE_{50}$ (1), $PEG_{113}PLD_{10}$ (2), $PEG_{113}PLD_{50}$ (3), $PEG_{113}PLD_{100}$ (4), $PEG_{113}PLE_{10}$ (5), $PEG_{113}PLE_{50}$ (6), $PEG_{113}PLE_{100}$ (7), PLD_{10} (8), PLD_{50} (9), PLD_{100} (10), PLE_{10} (11), PLE_{50} (12), $PLE_{50}PEG_{113}PLE_{50}$ (13), PLE_{100} (14)) on the surface of His_6-OPH. The molecular surface of the enzyme is depicted in gray. Molecules of PAAs are shown as green sticks. The entrances to the active sites of enzymes are highlighted with blue boxes.

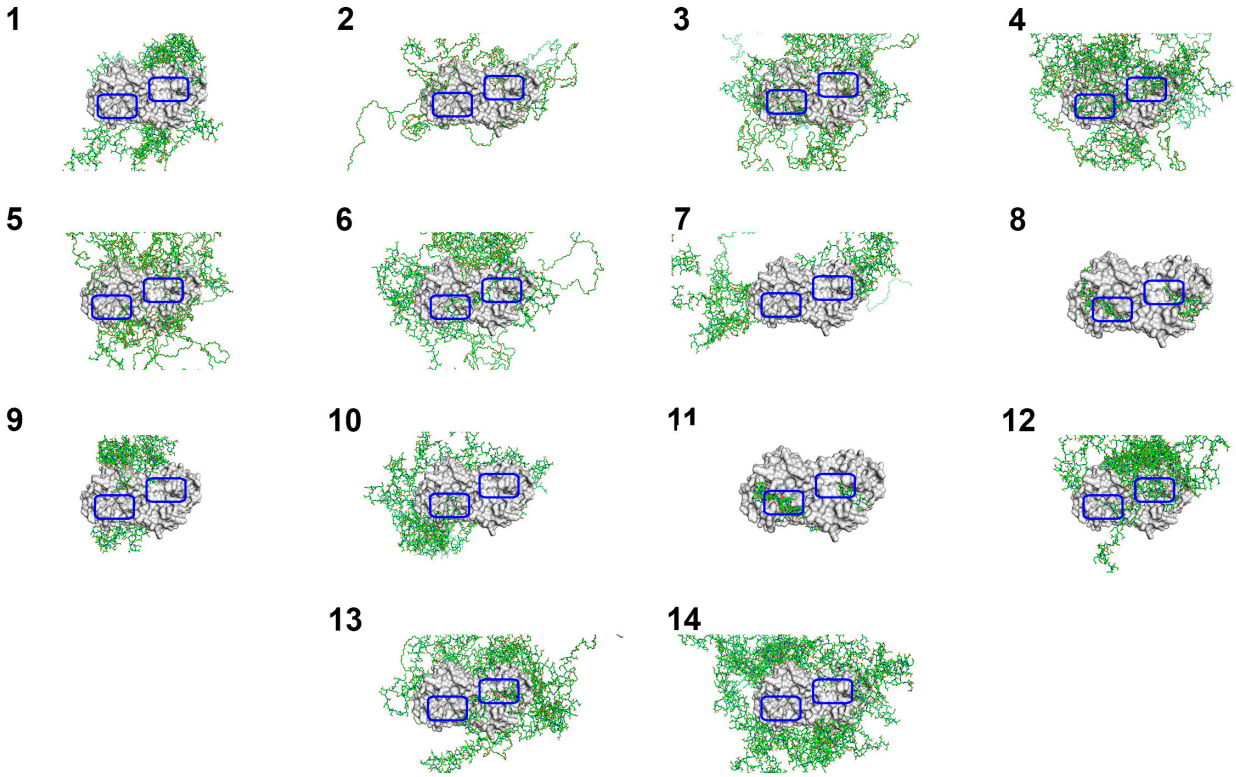


Figure S14. The localization of PAAs molecules ($PEG_{22}PLE_{50}$ (1), $PEG_{113}PLD_{10}$ (2), $PEG_{113}PLD_{50}$ (3), $PEG_{113}PLD_{100}$ (4), $PEG_{113}PLE_{10}$ (5), $PEG_{113}PLE_{50}$ (6), $PEG_{113}PLE_{100}$ (7), PLD_{10} (8), PLD_{50} (9), PLD_{100} (10), PLE_{10} (11), PLE_{50} (12), $PLE_{50}PEG_{113}PLE_{50}$ (13), PLE_{100} (14)) on the surface of NDM-1. The molecular surface of the enzyme is depicted in gray. Molecules of PAAs are shown as green sticks. The entrances to the active sites of enzymes are highlighted with blue boxes.

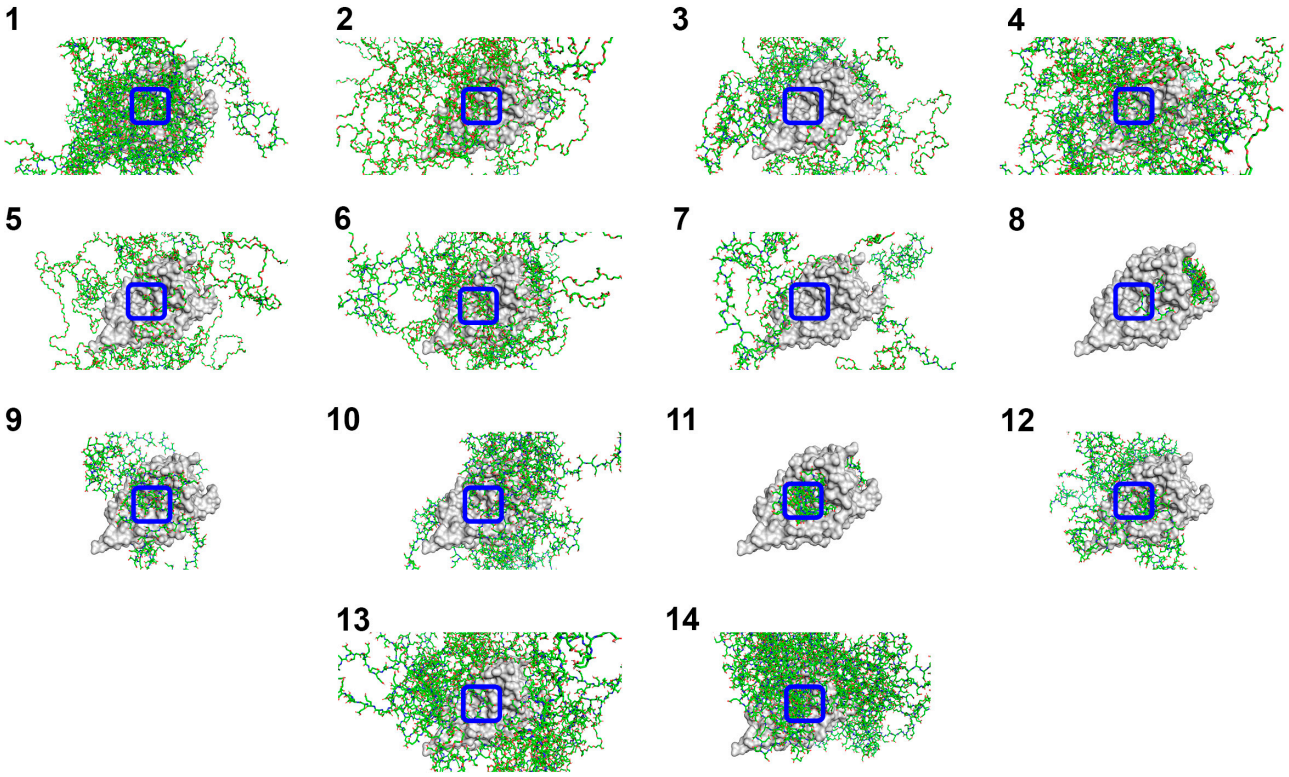


Figure S15. The localization of PAAs molecules ($PEG_{22}PLE_{50}$ (1), $PEG_{113}PLD_{10}$ (2), $PEG_{113}PLD_{50}$ (3), $PEG_{113}PLD_{100}$ (4), $PEG_{113}PLE_{10}$ (5), $PEG_{113}PLE_{50}$ (6), $PEG_{113}PLE_{100}$ (7), PLD_{10} (8), PLD_{50} (9), PLD_{100} (10), PLE_{10} (11), PLE_{50} (12), $PLE_{50}PEG_{113}PLE_{50}$ (13), PLE_{100} (14)) on the surface of MiM-1. The molecular surface of the enzyme is colored gray. Molecules of PAAs are shown as green sticks. The entrances to the active sites of enzymes are highlighted with blue boxes.

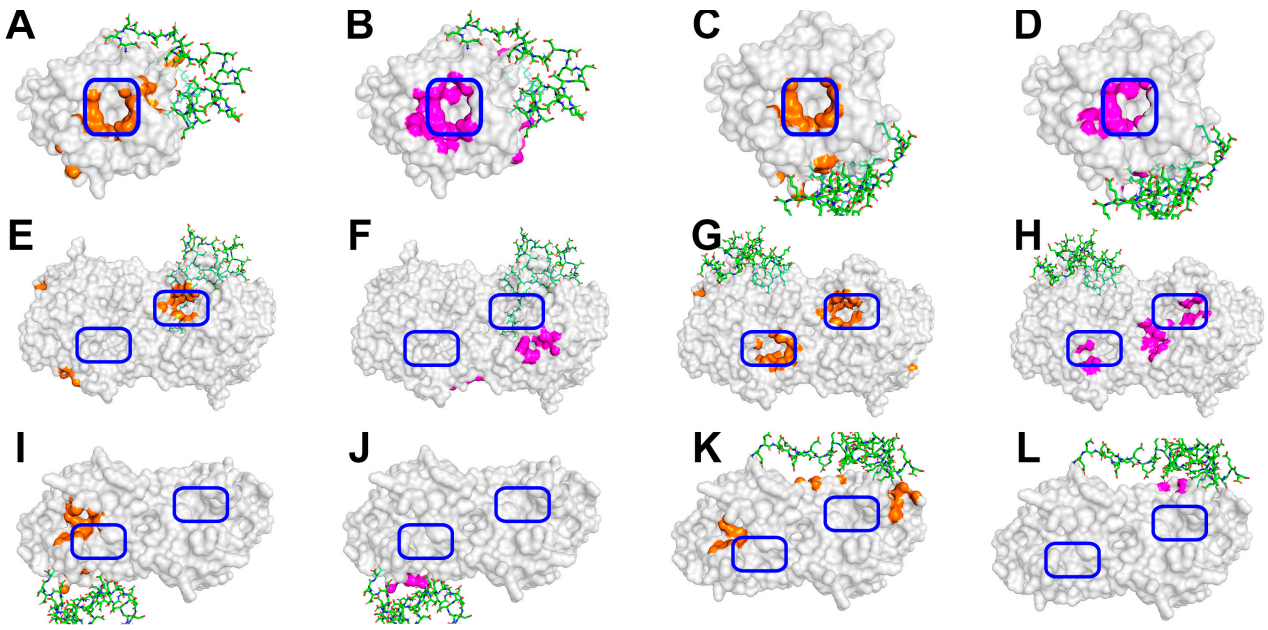


Figure S16. The localization of fungicides zineb (**A, C, E, G, I, K**) and clotrimazole (**B, D, F, H, J, L**) molecules on the surface of enzymes exhibiting lactonase activity AiiA (**A-D**), His_6-OPH (**E-H**), NDM-1 (**I-L**) combined with PLD_{50} (**A, B, E, F, I, J**) and PLE_{50} (**C, D, G, H, K, L**). The molecular surface of the enzymes is depicted in gray. The atoms located within 4 Å of any fungicide atom and the corresponding molecular surface of enzymes is colored orange (zineb) or purple (clotrimazole). Molecules of PAAs are shown as green sticks. The entrances to the active sites of enzymes are highlighted with blue boxes

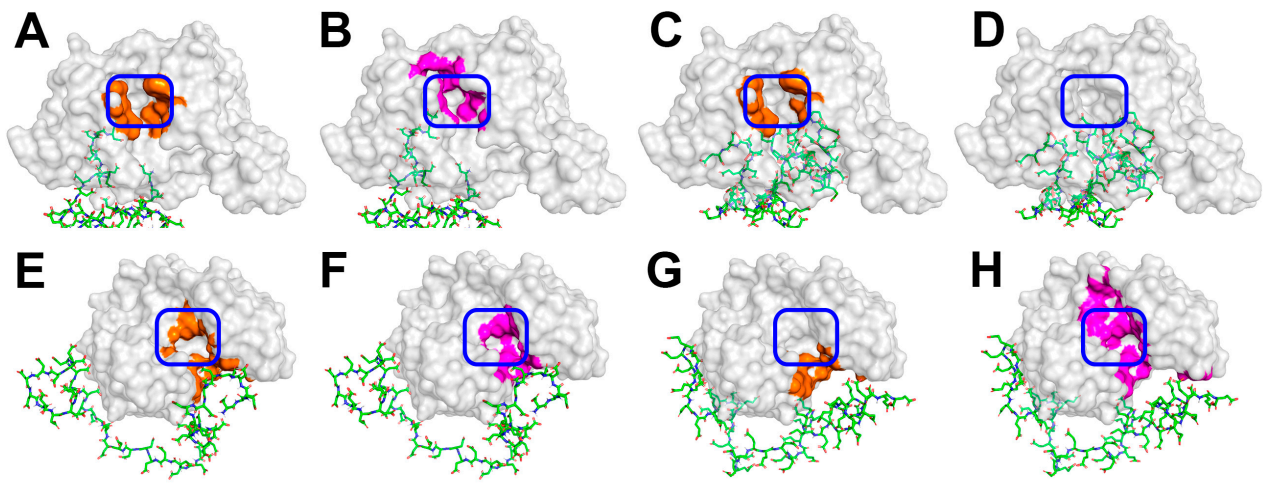


Figure S17. The localization of fungicides zineb **(A, C, E, G)** and clotrimazole (**B, D, F, H**) molecules on the surface of fungal cell wall degrading enzymes Bgy6 (**A-D**) and ChiC (**E-H**) combined with PLD_{50} (**A, B, E, F**) and PLE_{50} (**C, D, G, H**). The molecular surface of the enzymes is depicted in gray. The atoms located within 4 Å of any fungicide atom and the corresponding molecular surface of enzymes is colored orange (zineb) or purple (clotrimazole). Molecules of PAAs are shown as green sticks. The entrances to the active sites of enzymes are highlighted with blue boxes

References

8. Aslanli, A.; Domnin, M.; Stepanov, N.; Senko, O.; Efremenko, E. Action enhancement of antimicrobial peptides by their combination with enzymes hydrolyzing fungal quorum molecules. *Int. J. Biol. Macromol*. **2024**, *280*, 136066. https://doi.org/10.1016/j.ijbiomac.2024.136066.